TRENDS IN SCIENCES 2026; 23(4): 11840
https://doi.org/10.48048/tis.2026.11840 RESEARCH ARTICLE

Potential Effects of *Pseuderanthemum palatiferum* Extract on Inhibiting Adipogenesis and Promoting Lipolysis in 3T3-L1 Cell Line

Aekkaraj Nuallaong[1], Benjawan Dunkhunthod[2], Gordon Lowe[3], Kornsuda Thipart[4] and Tanaporn Hengpratom[5,*]

[1]*Division of Biological Science, Faculty of Science, Prince of Songkla University, Songkhla 90110, Thailand*
[2]*Thai Traditional Medicine Program, Faculty of Nursing and Allied Health Sciences, Phetchaburi Rajabhat University, Phetchaburi 76000, Thailand*
[3]*School of Pharmacy and Biomolecular Sciences, Faculty of Science, Liverpool John Moores University, Liverpool L3 3AF, United Kingdom*
[4]*Division of Health and Applied Sciences (Pharmacology Program), Faculty of Science, Prince of Songkla University, Songkhla 90110, Thailand*
[5]*Division of Health and Applied Sciences (Anatomy Program), Faculty of Science, Prince of Songkla University, Songkhla 90110, Thailand*

([*]Corresponding author's e-mail: tanaporn.he@psu.ac.th)

Received: 10 September 2025, Revised: 17 October 2025, Accepted: 24 October 2025, Published: 1 January 2026

Abstract

Obesity is a global health concern driven by excessive lipid accumulation and adipocyte dysfunction, requires therapeutic strategies that both inhibit fat formation and promote lipid degradation. This study investigated the dual anti-adipogenic and pro-lipolytic effects of *Pseuderanthemum palatiferum* leaf extract (PPE) in 3T3-L1 adipocytes. The phytochemical analysis of PPE performed by using gas chromatography-mass spectrometry (GC-MS) and Liquid chromatography-mass spectrometry (LC-MS). The findings revealed that GC-MS analysis of PPE identified 35 volatile compounds, with benzofuran (29.94%) as the major constituent. LC-MS detected 27 non-volatiles phytochemicals, including chlorogenic acid and p-coumaric acid. PPE exhibited no significant cytotoxic effects on 3T3-L1 preadipocytes at doses ranging from 50 - 150 µg/mL. At 150 µg/mL, PPE reduced lipid accumulation by 37.84% and increased glycerol release by 60.46%, indicating both an anti-adipogenic and a lipolytic properties. Gene expression analysis revealed that pre-treatment with 150 µg/mL of PPE promoted the upregulation of early adipogenic markers (C/EBPα, ACC1, FAS, and GLUT4) while downregulating markers associated with mature adipocytes (Adiponectin, AP2, and CD36), indicating interference with adipocyte differentiation and lipid synthesis. Additionally, PPE lowered intracellular reactive oxygen species, suggesting an antioxidative contribution to its anti-obesity action. Collectively, this study provides the first evidence that *P. palatiferum* exerts complementary regulation of adipogenesis and lipolysis in 3T3-L1 cells, offering new insight into its multi-target mechanisms and potential as a natural therapeutic candidate for obesity management.

Keywords: *Pseuderanthemum palatiferum*, Adipogenesis, Lipolysis, Adipocyte, 3T3-L1, Reactive oxygen species, Liquid chromatography-mass spectrometry, Gas chromatography-mass spectrometry

Introduction

Obesity is a condition of excessive body fat caused by an energy imbalance, influenced by factors such as diet, genetics, lifestyle, environment, hormonal disorders, certain medications, and psychological factors [1]. It is a global health challenge and is strongly associated with type 2 diabetes, cardiovascular diseases and can increase the relative risk of cancers with a hormonal influence such as breast cancer [2,3].

Conventional strategies for obesity prevention, such as caloric restriction and increased physical activity, often have limited long-term success, emphasizing the need for alternative therapeutic approaches that are both safe and effective [4]. Adipogenesis, the process by which precursor cells differentiate into mature adipocytes and this plays a pivotal role in the regulation of adipose tissue mass and energy homeostasis [5]. When this process becomes dysregulated, it contributes substantially to the development of obesity, a condition further aggravated by excessive oxidative stress and persistent inflammation. The interplay among these mechanisms underscores the therapeutic promise of natural compounds that can simultaneously regulate adipogenic and inflammatory pathways [6]. Conversely, lipolysis, the process by which triglycerides stored in adipocytes are hydrolyzed into free fatty acids and glycerol, is vital for energy mobilization [7]. While many studies have investigated these pathways independently, simultaneous assessment of adipogenesis and lipolysis provides a more comprehensive understanding of adipocyte metabolism and its therapeutic modulation. Clinically, an effective anti-obesity strategy should not only suppress the formation of new adipocytes but also enhance lipid mobilization from existing fat stores [7,8]. Thus, dual modulation of these processes provides a more comprehensive strategy for developing effective obesity treatments [9]. Plant-derived bioactive compounds, particularly those rich in polyphenols and antioxidants, have gained attention for their potential to modulate adipogenesis, enhance lipolysis, and counteract oxidative stress. One such promising source is *Pseuderanthemum palatiferum*, a medicinal plant traditionally used in Southeast Asia possesses a wide range of pharmacological activities, including anti-diabetic, anti-inflammatory, anticancer, and antioxidant properties effects, which is largely attributed to its rich phytochemical content. [10-13]. However, despite extensive studies on its anti-inflammatory and anti-diabetic effects, its potential role in regulating adipocyte metabolism, particularly through dual modulation of adipogenesis and lipolysis in 3T3-L1 cells remains largely unexplored. To address this knowledge gap, this study we investigate the phytochemical composition and dual anti-obesity potential of *P.palatiferum* extract (PPE). Comprehensive chemical profiling was performed using gas chromatography–mass spectrometry (GC–MS) and liquid chromatography–tandem mass spectrometry (LC–MS/MS). The biological activity of PPE was then evaluated in 3T3-L1 preadipocytes, focusing on its effects on adipogenesis, lipolysis, and oxidative balance. By elucidating these mechanisms, this study provides new evidence supporting PPE as a multifunctional botanical candidate for obesity management.

Materials and methods

Plant preparation and extraction

Pseuderanthemum palatiferum fresh leaves were purchased from the vendor in Yasothon province, Thailand. The collected plants (a voucher specimen: BKF 174009) were identified by Dr. Kongkanda Chayamarit, The forest herbarium, Department of National Parks, Wildlife and Plant Conservation, Bangkok, Thailand. Based on previous pharmacognostic evaluation [14], the leaves are ovate to elliptic, 5 - 10 cm long and 2 - 5 cm wide, with an acuminate apex, entire margins, dark green upper surface, and pale green, slightly pubescent lower surface. Microscopic examination revealed an upper epidermis with polygonal cells and glandular trichomes, palisade and spongy mesophyll, vascular bundles, and diacytic stomata on the lower epidermis. Physicochemical parameters confirmed moisture content, ash values, and extractive values within standard limits, while preliminary phytochemical screening indicated the presence of phenolics, flavonoids, tannins, and alkaloids [14,15]. The *Pseuderanthemum palatiferum* extract (PPE) was prepared following the method previously described [16]. Briefly, fresh leaves were washed thoroughly to remove the debris and cut to small pieces, then blended with 95% ethanol. The extract was centrifuged at 3,500 g at 4 °C for 10 min and the supernatant was filtered through Whatman Grade No. 1. The ethanolic extract was concentrated using a rotary vacuum evaporator and then lyophilized (Buchi Labortechnik AG, Flawil, Switzerland) to obtain a powder. Following these 40 g of the powder was further extracted using a liquid–liquid extraction (hexane and water (1:1)) technique to ease the separation between less and high polarity. The water fraction (high polarity) was collected, then centrifuged at 14,000 g at 4 °C for

10 min, evaporated, and lyophilized to obtain an extract compound (PPE; 32.71 g). The PPE was stored at −20 °C prior to experimental use.

Gas Chromatography - Mass Spectrometry (GC-MS) analysis

The analysis of PPE volatile compounds was performed using GC-MS. The GC-MS analysis was carried out in a combined Agilent 7890A gas chromatograph system and Agilent 7000B mass spectrophotometer, fitted with DB-WAX Ultra Inert GC columns (60 m×0.25 mm, 0.25 µm). For GC-MS detection, an electron ionization system with an ionization energy of 70 eV was used, and the carrier gas was helium which was delivered at a rate of 1.0 mL/min. A 2 µL liquid sample was injected and performed in split mode adjusted to 5:1. The column oven temperature was programmed to rise from 60 - 200 °C at 3 °C/min, then it was held at 200 °C for 3 min. It was raised to 250 °C at a rate of 5 °C/min for 20 min. The relative percentage of PPE identified components was calculated as percentage by peak area normalization. A tentative identification of the compounds was performed based on the comparison of their relative retention time and mass spectra with those of the NIST MS Search 2.0 Library.

Liquid Chromatography- Mass Spectrometry (LC-MS) analysis

The analysis for polyphenols was performed on the Dionex Ultimate 3,000 UHPLC system (Dionex, USA) coupled to a micrOTOF-Q II mass spectrometer (Bruker, Germany), equipped with electrospray source (ESI) and operated in a negative-ion mode. The chromatographic separation was performed using a Zorbax SB-C18 column (250×4.6 mm^2×3.5 µm) at 35 °C. The sample was prepared at concentration 20 mg/mL in methanol. A 5 µL amount was delivered to the column. The solvent was delivered at a flow rate of 0.8 mL/min. The mobile phase A included deionized water containing 0.1% formic acid; the mobile phase B included acetonitrile containing 0.1% formic acid. The analysis was performed using a solvent gradient programmed as follows: 10% B and holding for 5 min; increase to 40% B at 40 min; increase to 80% at 55 min, and hold it until 65 min. Next, the solvent was reduced to 10% B in 2 min and held until the run ended at 70 min. The eluted composition was detected in the scanning mode with mass range from 50 - 1,500 m/z. The Q-TOF settings were as follows: Nebulizer nitrogen gas with 180 °C temperature, 2 bar pressure, drying gas of 8 L/min, capillary voltage was set to 4.5 kV. The LC-QTOF data were collected and process by Compass 1.3 software (Bruker, Germany). Twelve target compounds were identified using Bruker Quant Analysis software (DIFFRAC.DQUANT version 2.0, Bruker Daltonik GmbH). The major constituents of PPE were quantified using corresponding reference standards, with calibration curves demonstrating excellent linearity (chlorogenic acid, R^2 = 0.9884; p-coumaric acid, R^2 = 0.9979) over a concentration range of 5 - 250 µg/mL. These results ensure reliable identification and quantification, in accordance with standard analytical guidelines.

Cell culture and differentiation

3T3-L1 preadipocytes were purchased from the American Type Culture Collection (ATCC, USA). The preadipocytes cell were cultured in Dulbecco's Modified Eagle's Medium-High glucose supplemented with 10% fetal bovine serum (FBS; v/v) (Thermo Fisher Scientific, USA). Cells were grown under CO_2 in an incubator (37 °C and 5% CO_2). Preadipocytes were seeded at a density of 7.5×10^4 cells/mL in a 6-well culture plate. Two days after cells reached confluence, cells were differentiated with 10% FBS DMEM contain MDI (0.5 µM isobutylmethylxanthine IBMX, 5 µM dexamethasone and 0.5 µg/mL insulin) (Sigma-Aldrich, USA). Two days later the medium was replaced using 10% FBS DMEM containing 5 µg/mL insulin. This solution was changed every two days over 8 days period. At the completion of induction, cells become rounded and exhibited the large lipid droplets occupy most of the cytoplasm. To investigate the effects of PPE on inhibiting adipocyte formation, the inducing medium contained various concentration of PPE from 25 - 150 µg/mL. The medium was changed every 2 days until end of the induction process. The vehicle control was treated with 0.2% DMSO (vehicle control) in the same medium without PPE **Figure 1**.

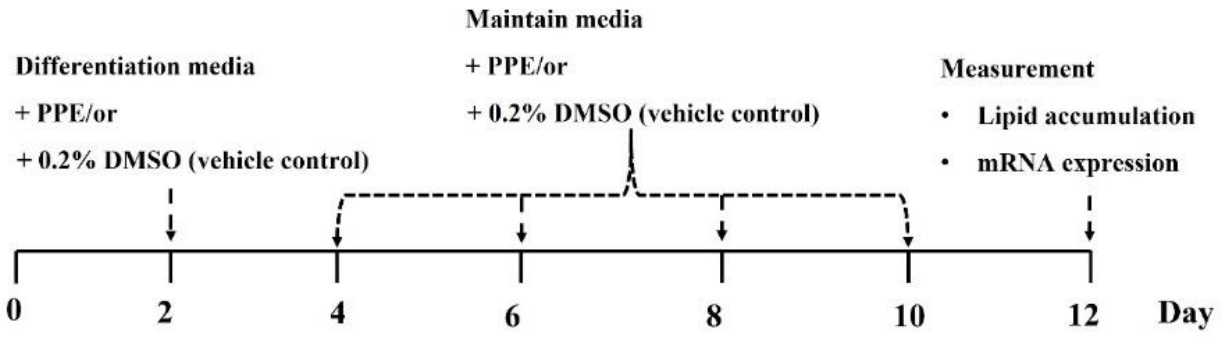

Figure 1 Cell culture and cell differentiation process.

Cell viability

The viability of 3T3-L1 cells was assessed by MTT (Sigma-Aldrich, USA) colorimetric assay. The 3T3-L1 cells were grown in 96-well plate at a density of 5×10^3 cells/well and incubated overnight. After the incubation, the cells were exposed to various concentrations of PPE (0 - 800 µg/mL) for 48 h. Cells treated with 0.2 %v/v DMSO were used as vehicle controls. After 48 h, MTT (0.5 mg/mL) dye solution was added in each well and further incubated at 37 °C, 5% CO_2 for 3 h. The solution was removed and 100 µL/well of DMSO (Loba, India) was added to dissolve the formazan crystals for 10 min. In this assay, the ability of metabolically active cells to convert MTT into a blue formazan product was measured and its absorbance was recorded at 540 nm using a microplate reader (Biotek, USA). The percentage of cell viability was calculated by the following equation (% cell viability = (absorbance of test group/ absorbance of control group) ×100). The half maximal inhibitory concentration (IC_{50}) of PPE were calculated from a dose response curve using linear regression analysis.

Lipid staining and quantification

The amount of lipid accumulation in the cells was assessed by the Oil-Red O (Sigma-Aldrich, USA) staining technique. The 3T3-L1 differentiated cells were washed with 1X PBS twice, then fixed with 10% formalin for 30 min at room temperature. The fixed cells were washed with DI water twice and stained with 60% Oil Red O working solution for 30 min. Following this step, the dye was removed, and the stained cells were washed with distilled water (DI) twice before double stain with hematoxylin solution (this double staining is only for lipid qualification). Next, the hematoxylin (Sigma-Aldrich, USA) dye solution was removed, and the cells were washed with DI twice. The lipid droplets were visualized, and an image was taken under the inverted microscope (Evos XL core). To quantify the amount of intracellular lipid, the Oil-Red-O dye was extracted by 100% of the isopropanol for 10 min, then the extracted dye was transferred to 96 wells plate and the absorbance was measured at 520 nm.

Glycerol release level

The amount of glycerol level was measured to study the lipolysis effects of PPE. The glycerol released in the culture media was detected by lipolysis assay kit (Abcam, UK). 3T3-L1 were grown in 24 well plates (at density 5×10^4 cells/well) and differentiated to mature adipocytes as described previously. Initially, the cells were gently washed twice with a washing buffer and replaced by the lipolysis assay buffer. Mature adipocytes were pre-incubated with 50 - 150 ug/mL of PPE for 24 h, then the medium was replaced. To encourage of the lipolysis and releasing of the glycerol in the medium, the cells was incubated with 100 nM of isoproterenol (lipolysis inducer) for 3 h. The glycerol released to the medium was collected and transferred to 96 well plate and measured by colorimetric absorbance read at 570 nm. A standard curve was prepared, using a standard solution of glycerol at concentration of 0 - 10 nmol (($y = 0.1584x + 0.0404$, $R^2 = 0.9973$); **Supplementary data 1**. Sample readings were applied to the standard curve to get glycerol amount in the samples

Real time PCR analysis

RNA extraction and cDNA synthesis

Total RNA was extracted from 3T3-L1 adipocytes using the EXM3000 Series Nucleic Acid Isolation System (Zybio, China) by Nucleic Acid Extraction Kit (Zybio, China) with the manufacturers recommended. The extracted nucleic acids were treated with DNase I (Invitrogen, Thermo Fisher Scientific, USA) to remove contaminating genomic DNA. The concentration and purity of RNA were determined using a NanoDrop Spectrophotometer (Invitrogen, Thermo Fisher Scientific, USA). RNA integrity was further assessed by electrophoresis on a 1% agarose gel at 135 V for 20 min. High-quality RNA samples were adjusted to a final concentration of 200 ng and subsequently reverse-transcribed into complementary DNA (cDNA) using the Revert Aid First Strand cDNA Synthesis Kit (Thermo Fisher Scientific, USA) with Oligo(dT)$_{18}$ primers, according to the manufacturer's protocol.

The quantitative real-time PCR assay

Gradient PCR was performed to determine the optimal annealing temperature for each primer using a real-time qPCR instrument with a gradient function. The quantitative gene expression analysis was subsequently carried out on the Bio-Rad CFX Connect™ Real-Time PCR Detection System (Bio-Rad Laboratories, USA) with a total volume of 20 µL containing 10 µL 2× SensiFAST SYBR® No-ROX Mix (Bioline, Canada), 0.8 µL of each primer (final concentration 400 nM), 1 µL cDNA (dilution 1:20), and nuclease-free water. The thermal cycling conditions were set as follows: Initial denaturation at 95 °C for 2 min, followed by 40 cycles of denaturation at 95 °C for 5 s, annealing at the primer-specific annealing temperature (determined by gradient PCR; show in **Supplementary data 2** for 10 s, and extension 72°C 20 s coupled with plate reading. No template controls (NTCs) were used as negative controls and each reaction was done with three technical replicates. The fold change in expression level of Adipogenic target gene was normalized against β-actin1 of the same sample using the $2^{-\Delta\Delta Cq}$ method [17]. The quality and specificity of each primer pair was verified by visualization on agarose gel electrophoresis as well as by a melting curve analysis during the RT-qPCR assay (between 65 and 95 °C with an increment of 0.5 °C).

Reactive Oxygen Species (ROS)

ROS levels were determined using the fluorescent probe, DCFH-DA (Sigma-Aldrich, USA) in accordance with a method described by Dunkhunthod *et al*. [18] with some modification [18]. Briefly, Cells were seeded at a density of 5× 10^3 cells/well in a 96-well black, clear-bottom plate and incubated for 24 h. Subsequently, cells were differentiated and pre-treated with PPE at concentrations of 50, 100 and 150 µg/mL for 10 days. After treatment, the culture medium was removed, and cells were incubated with 3 mM N-acetylcysteine (NAC) (Sigma-Aldrich, USA) for 3 h. Following incubation, the medium was removed, and cells were loaded with 20 M DCFH-DA in Hanks' Balanced Salt Solution (Thermo Fisher Scientific, USA) at 37 °C for 30 min in the dark. Afterward, cells were washed with PBS, and fluorescence intensity was measured using a Biotek Synergy HT Microplate Reader (Biotek, USA) at an excitation/emission wavelength of 485/528 nm. The percentage of fluorescence intensity was calculated using the following formula: Fluorescence intensity (%) = (fluorescence intensity of test group/ fluorescence intensity of control group)×100.

Statistical analysis

All data were analysis using SPSS version 23 (SPSS Inc., Chicago, IL, USA). One-way analysis of variance (ANOVA) was used to assess differences among the groups, Tukey's Honestly Significant Difference (HSD) test was conducted as a post hoc analysis to determine specific group differences. All data are presented as mean ± standard deviation (SD) from at least three independent experiments. The statistically significant was considered at p - value < 0.05.

Results and discussion

Phytochemical compositions of PPE

Separation and identification of volatile compounds of PPE was performed using GC-MS. A total of 35 compounds were identified and the chromatogram is presented in **Figure 2**. Benzofuran, 2,3-dihydro- was found to be the highest concentration

(29.94%). **Supplementary 3** provides a list of compounds that were found in a trace amount. The LC-MS chromatogram reveals a total of 27 compounds found in PPE. The peaks in the chromatograms were identified as chlorogenic acid and p-coumaric acid by comparing retention times with 15 standard compounds **Figure 3**. The chlorogenic acid and p-coumaric acid was found in PPE with a concentration of 1.23 and 0.47 mg/g extract, respectively **Table 1.**

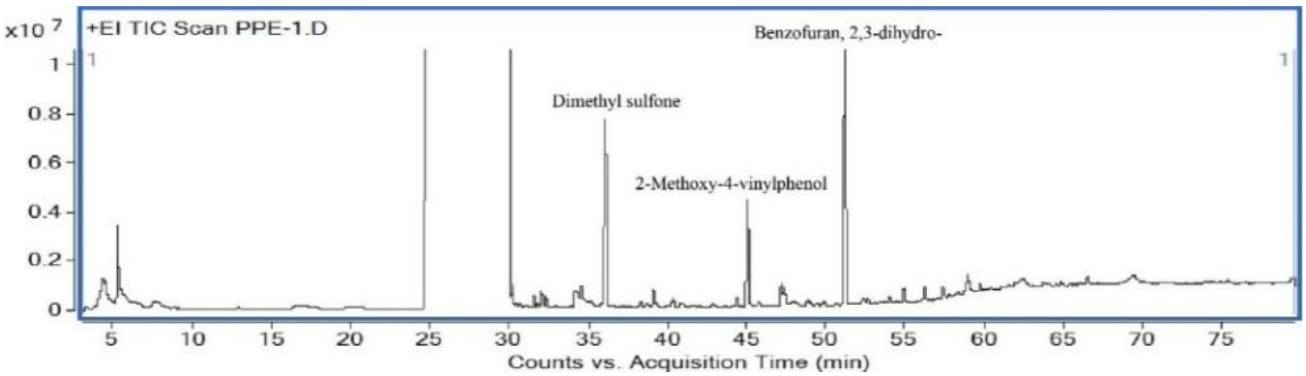

Figure 2 Gas chromatography/mass spectrometry (GC/MS) chromatogram of PPE. GC-MS analysis was conducted using an Agilent system with a DB-WAX column. Samples (2 µL) were injected in split mode (5:1) onto a DB-WAX Ultra Inert column, with helium as the carrier gas at 1.0 mL/min. The oven temperature was programmed from 60 - 200 °C at 3 °C/min (held for 3 min), then increased to 250 at 5 °C/min and held for 20 min.

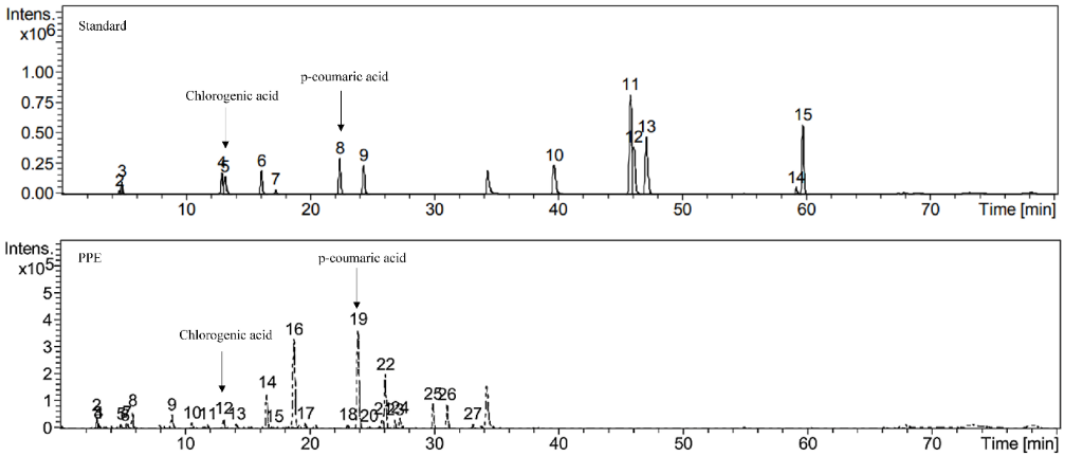

Figure 3 Liquid chromatography quadrupole time of flight mass spectrometry (LC-QTOF/MS) chromatogram of PPE compared to the standard. Phenolic compounds were analyzed using a Dionex Ultimate 3000 UHPLC with a Zorbax SB-C18 column (35 °C, 0.8 mL/min, 10 µL injection). The mobile phases were water with 0.1% formic acid (A) and acetonitrile with 0.1% formic acid (B) under a programmed gradient. Detection was done by micrOTOF-Q II MS in negative ESI mode, scanning 50 - 1500 m/z.

Table 1 Liquid chromatography quadrupole time of flight mass spectrometry (LC-QTOF/MS) profile of PPE.

Compound	Retention time	Base peak (m/z)	Area	Concentration (ppm)
Chlorogenic acid	13.1	353	343995.60	24.55
P-coumaric acid	22.4	163	5287.80	9.34

The cytotoxic effects of PPE

The MTT assay were used to evaluate the effects of PPE on cell viability of 3T3-L1 cells. The 3T3-L1 cells were incubated with various concentration of PPE ranging from 50 - 800 µg/mL for 48 h **Figure 4**. There was no significant effect on cell viability at dose of PPE which were less than 150 µg/mL. However, at the doses of PPE above 250 µg/mL there was a significant decrease in cell viability ($p < 0.05$) compared to the untreated control group and the vehicle control (0.2% DMSO). The IC_{50} of the PPE for 3T3-L1 cells (904.614 ± 10.559 µg/mL) was delivered from a dose response curve using linear regression analysis. Based on this result a concentration of PPE between 50, 100 and 150 µg/mL were selected for further investigation.

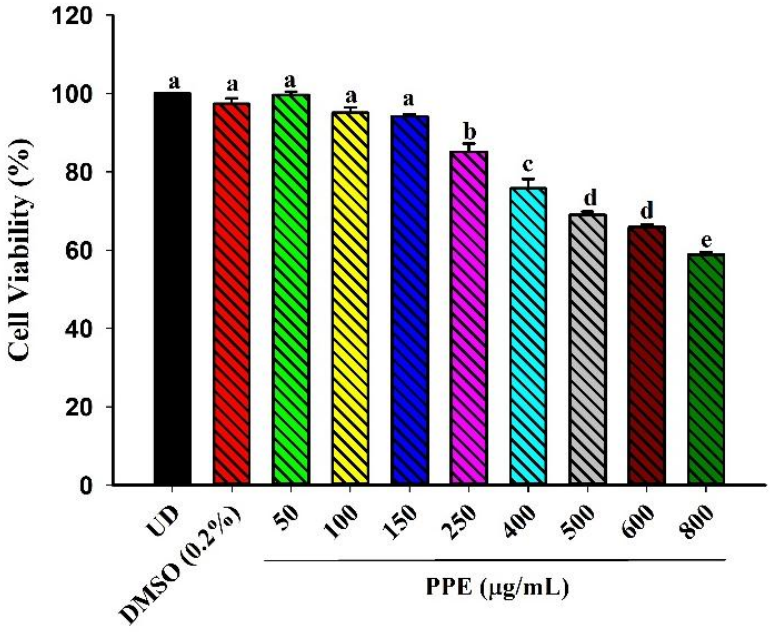

Figure 4 Cytotoxicity effects of PPE at concentration ranging from 50 - 800 µg/mL against 3T3-L1 cells for 48 h. Undifferentiated cells (pre-adipocytes), DMSO (0.2%) = Undifferentiated cells (pre-adipocytes) + 0.2% DMSO (vehicle control), PPE 50 - 800 = Undifferentiated cells (pre-adipocytes) + *P. palatiferum* extract at dose at dose 50 - 800 µg/mL. The results were expressed as mean ± SD. The different letters a to e showed statistically significant differences at $p < 0.05$ (ANOVA with Tukey's HSD post hoc test).

The effects of PPE on adipogenesis activity

Adipogenesis is the process in which precursor cells differentiate into adipocytes, specialized cells responsible for lipid storage. 3T3-L1 cells were differentiated together treated with 50, 100 and 150 µg/mL of PPE. Oil- Red-O lipid staining dye were used to visualize and determine an intracellular lipid accumulation. The effects of the PPE on lipid accumulation are shown in **Figure 5(A)** (lipid accumulation level) and **Figure 5(B)** (morphology of cells). The differentiated cells showed a more prominent fat droplet formation (red color) compared to the undifferentiated cells (pre-adipocytes). While cells treated with PPE reduced lipid droplet formation compared to the non-treated differentiated cells. The results are consistence with the lipid accumulation level **Figure 5**. The percentage of lipid level of PPE at concentration of 50, 100 and 150 µg/mL significantly ($p < 0.05$) reduced by 25.19 ± 7.34% (P = 0.000015, compared to vehicle control), 28.59 ± 1.99% (P = 0.000003, compared to vehicle control), and 37.84 ± 3.37% (P = 0.0000000604, compared to vehicle control), respectively compared to the non-treated differentiated cells. These findings implied that PPE at concentration of 50, 100 and 150 µg/mL may interfere during adipogenesis.

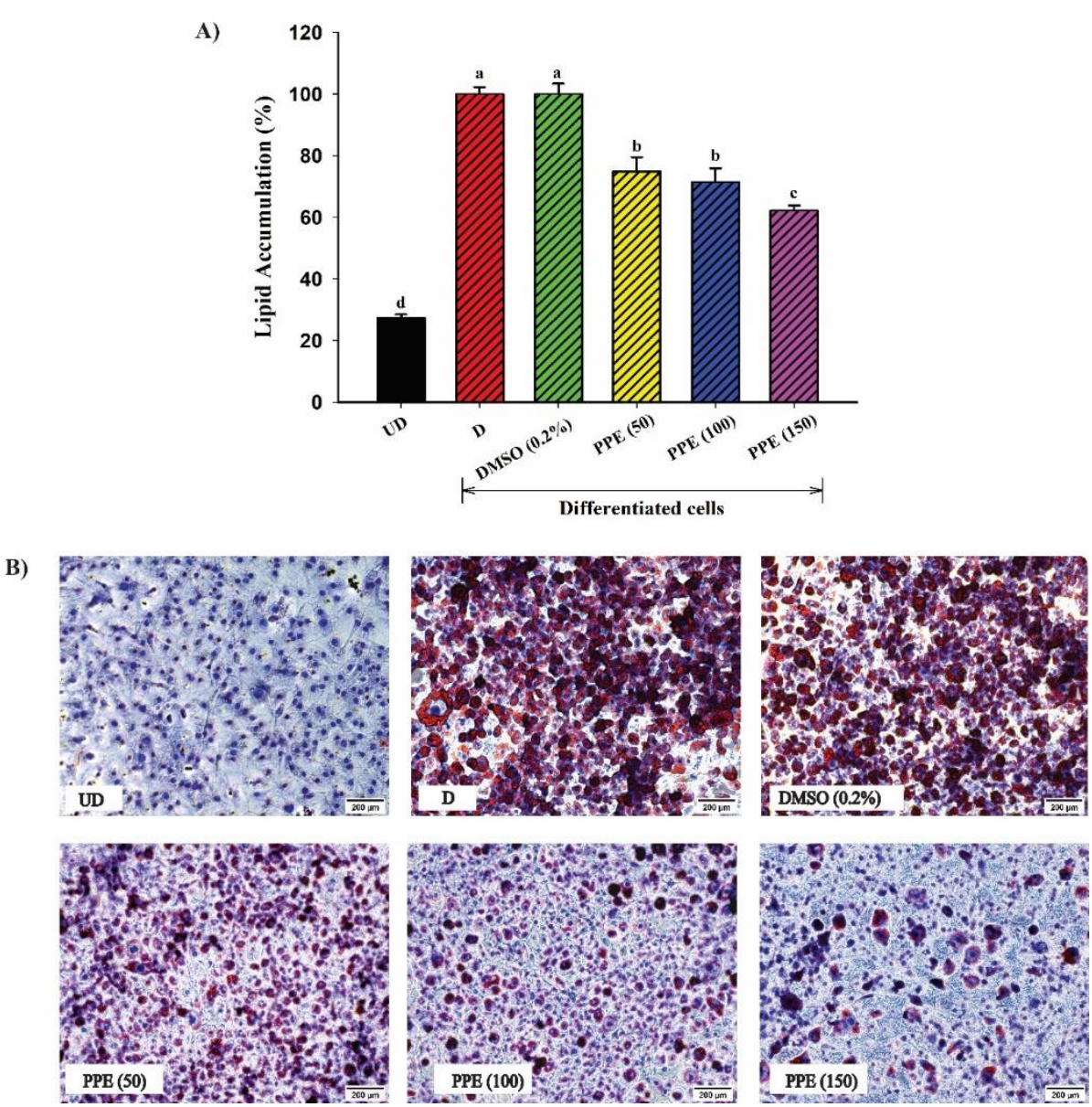

Figure 5 The effects of PPE on adipogenesis activity. (A) Percentage of lipid accumulation level (B) Morphology of cells counterstained with Oil-Red-O (red color = lipid droplets) and hematoxylin (blue to purple color = nuclei). UD = Undifferentiated cells (pre-adipocytes), D = Differentiated cells (adipocytes), DMSO (0.2%) = Differentiated cells (adipocytes) + DMSO (0.2%); vehicle control, PPE 50 - 150 µg/mL = Differentiated cells (adipocytes) + *P. palatiferum* extract at dose 50, 100 and 150 µg/mL. The results were expressed as mean ± SD. The different letters a to d showed statistically significant differences at $p < 0.05$ (ANOVA with Tukey's HSD post hoc test).

The effect of PPE on lipolysis activity

Lipolysis is a catabolic pathway by which triglycerides are converted into glycerol and free fatty acids. 3T3-L1 cells were differentiated into mature adipocytes, after that the mature adipocyte were treated with PPE at 50, 100 and 150 µg/mL for 24 h. The lipolysis effects of the PPE are shown in **Figure 6**. The glycerol release of the differentiated cells significantly ($p < 0.05$) increased compared to the undifferentiated cells. Whilst cells treated with PPE at 100 and 150 µg/mL significantly ($p < 0.05$) increased of glycerol released level by 50.09 ± 15.59% (P = 0.011785, compared to vehicle control) and 60.46 ± 12.89% (P = 0.003268, compared to vehicle control) respectively, compared to the differentiated cells. The results revealed

that PPE at concentration of 100 and 150 µg/mL treated mature adipocyte for 24 h enhanced lipolytic activity.

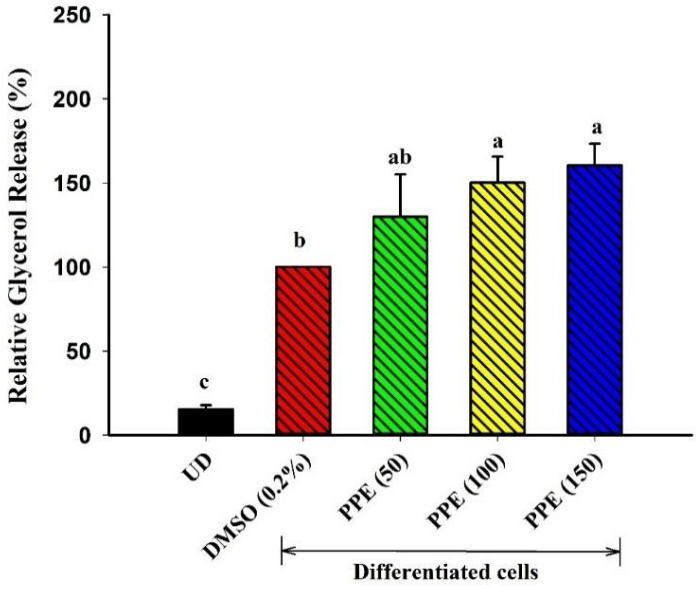

Figure 6 Effect of PPE on lipolysis activity. UD = Undifferentiated cells (pre-adipocytes), DMSO (0.2%) = Differentiated cells (adipocytes) + DMSO (0.2%); vehicle control, PPE 50 - 150 µg/mL = Differentiated cells (adipocytes) + *P. palatiferum* extract at dose 50, 100 and 150 µg/mL. The results were expressed as mean ± SD. The different letters a to c showed statistically significant differences at $p < 0.05$ (ANOVA with Tukey's HSD post hoc test).

The effect of PPE on mRNA expression of genes involved in lipid metabolism

Adipogenesis is a very complex process which is regulated by transcription factors and cell signaling pathways. In this study mRNA transcriptional for C/EBPα, ACC1, FAS, GLUT4, adiponectin, FABP4, and CD36 were assessed in 3T3-L1 cells **Figures 7(A) - 7(G)**. Cells were differentiated and treated with PPE at 50, 100 and 150 µg/mL for 10 days. C/EBPα plays a crucial role in initiating and sustaining adipogenesis, the result revealed that the differentiated cells was significantly decreased ($p < 0.05$) of C/EBPα levels compared to undifferentiated cells. Similarly, PPE-treated cells at concentrations of 100 and 150 µg/mL exhibited a significant increase ($p < 0.05$) in C/EBPα levels. ACC1 and FAS, key enzymes involved in de novo lipogenesis, and were significantly elevated ($p < 0.05$) in PPE-treated cells at 150 µg/mL compared to the non-treated differentiated cells. An increased expression of GLUT4, a key glucose transporter involved in insulin-mediated glucose uptake, was also observed in both undifferentiated and PPE-treated cells. In contrast, adiponectin and FABP4 are well-established markers of mature adipocytes and were upregulated in differentiated cells. Notably, pre-treatment with PPE resulted in a marked downregulation of adiponectin and FABP4 expression. Moreover, overexpression of CD36, which facilitates the uptake of fatty acids and oxidized low-density lipoprotein (oxLDL) was observed in differentiated cells, whereas treatment with PPE at concentrations of 50 - 150 µg/mL significantly decreased CD36 expression. This study demonstrates that PPE modulates the expression of key genes involved in adipogenesis in 3T3-L1 cells. PPE treatment notably suppressed the expression of mature adipocyte markers such as adiponectin, FABP4, and CD36, while upregulating early adipogenic markers including C/EBPα, ACC1, FAS, and GLUT4. This dual effect may involve oxidative stress modulation, as reactive oxygen species (ROS) are required for full adipocyte maturation. PPE's antioxidant activity could reduce ROS, disrupting redox-sensitive pathways, limiting late-stage adipocyte gene expression and lipid accumulation. Further studies on ROS are needed to confirm this mechanism.

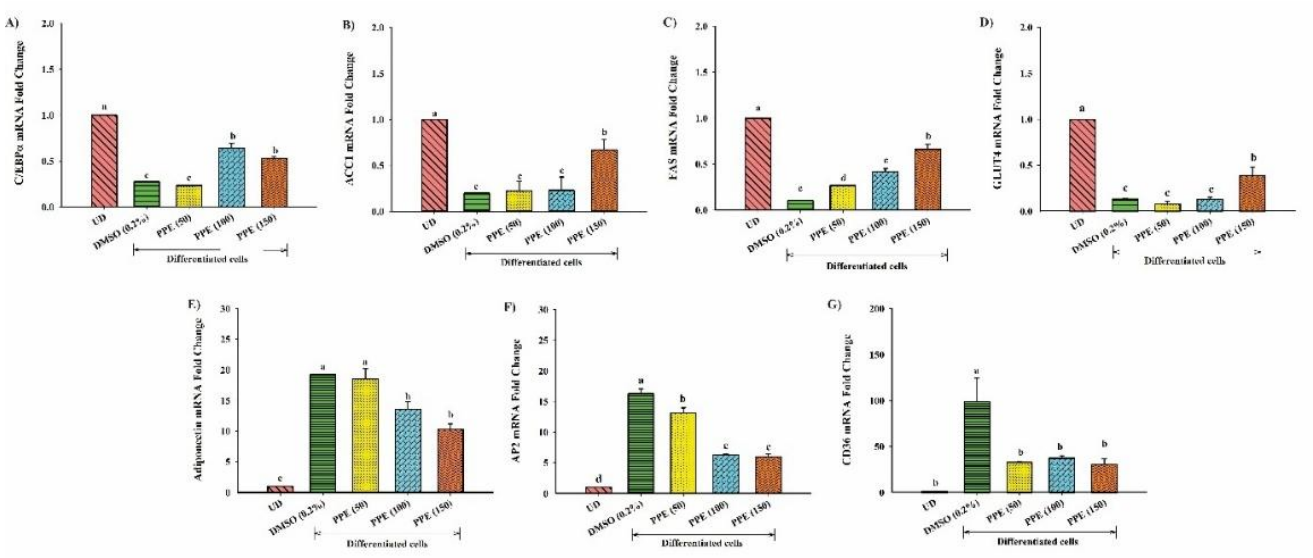

Figure 7 Effect of PPE on adipogenesis gene expressions in 3T3-L1 cells; quantified by RT-qPCR. An expression level of mRNA (A) C/EBPα, (B) ACC1, (C) FAS, (D) GLUT4, (E) Adiponectin, (F) AP2, and (G) CD36. Gene expression levels were normalized to the housekeeping gene (β-Actin). Bars represent mean ± SD; expressed using the 2−ΔΔCt method. UD = Undifferentiated cells (pre-adipocytes), DMSO (0.2%) = Differentiated cells (adipocytes) + DMSO (0.2%); vehicle control, PPE 50 - 150 µg/mL = Differentiated cells (adipocytes) + *P. palatiferum* extract at dose 50, 100 and 150 µg/mL. The results were expressed as mean ± SD. The different letters a to d showed statistically significant differences at $p < 0.05$ (ANOVA with Tukey's HSD post hoc test).

The effect of PPE on ROS production

Cells were differentiated and subsequently pretreated with PPE at concentrations of 50, 100 and 150 µg/mL for 10 days. Intracellular ROS level was assessed in undifferentiated cells (UD), differentiated cells with 0.2 %v/v DMSO (D), 3 mM of N-acetyl cysteine (NAC; positive control), and 50, 100 and 150 µg/mL of PPE. The treatment with NAC was very effective, providing approximately 90% protection compared to the differentiated 3T3-L1 cells. The PPE treatment displayed a dose dependent protection with a 150 µg/mL providing 48.44% protection **Figure 8**. However, further studies are required to determine whether PPE reduces ROS by directly scavenging radicals or by modulating cellular antioxidant pathways.

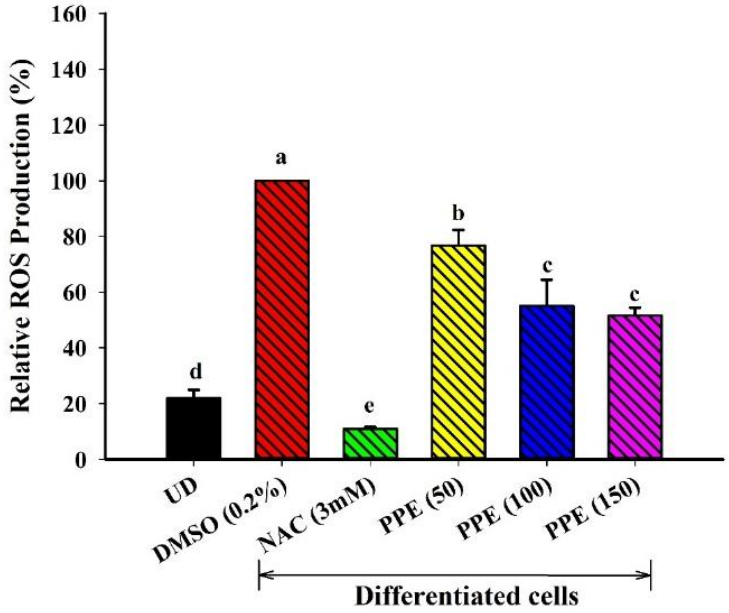

Figure 8 The effects of PPE on intracellular reactive oxygen species (ROS) in 3T3-L1 cells. The cells were pretreated with NAC at 3 mM or PPE at 50, 100 and 200 µg/mL. UD = undifferentiated cells (pre-adipocytes), DMSO (0.2%) = Differentiated cells (adipocytes) + DMSO (0.2%); vehicle control, PPE 50 - 150 µg/mL = Differentiated cells (adipocytes) + *P. palatiferum* extract at dose 50, 100 and 150 µg/mL. The results were expressed as mean ± SD. The different letters a to e showed statistically significant differences at $p < 0.05$ (ANOVA with Tukey's HSD post hoc test).

Discussion

Adipocytes have a central role for glucose and lipid metabolism in the body. An increase in adipocyte size and number is linked to metabolic dysfunction and obesity-related diseases [19]. Thus, controlling the size and number of adipocytes could possibly be a therapeutic approach for obesity. Recently, scientific research has highlighted the anti-obesity effects derived from natural sources through several mechanism include appetite suppression, metabolic and thermogenic stimulation, inhibition of pancreatic lipase and amylase, enhancement of insulin sensitivity, inhibition of adipogenesis, and induction of adipocyte apoptosis [20]. This study investigated the chemical composition and anti-obesity effects of *Pseuderanthemum palatiferum* leaves extract (PPE), highlighting its potential as a natural modulator of adipogenesis and lipolysis. The concentrations of PPE used in this study (50 - 150 µg/mL) were selected based on cytotoxicity and are considered physiologically relevant. Previous study demonstrated that PPE at 10 - 200 µg/mL significantly suppressed nitric oxide production and downregulated iNOS and COX-2 expression in RAW264.7 macrophages, confirming its antioxidant and anti-inflammatory activities [15]. Consistently, oral administration of PPE at 250 - 750 mg/kg effectively reduced both acute and chronic inflammation rats [13], while doses of 500 - 1,000 mg/kg improved lipid profiles in diabetic rats by elevating HDL levels and reducing total cholesterol, triglycerides, and low density lipoprotein (LDL) [21]. Furthermore, acute and chronic toxicity assessments established that PPE is safe at doses up to 2,000 mg/kg and 1,000 mg/kg/day, respectively [22]. These values correspond to the concentrations applied *in vitro*, supporting their pharmacological plausibility under physiological conditions. GC-MS analysis revealed that PPE presents a variety of volatile compounds, with benzofuran, 2,3-dihydro- being the most abundant. These compounds have previously been associated with antioxidant and anti-inflammatory properties [23-25]. Complementarily, LC-MS/MS profiling demonstrated the presence of two phenolic compounds, notably chlorogenic acid and p-coumaric acid. Similarly, previous study revealed that the phenolic contents in *P. palatiferum* ethanolic extract quantified using HPLC-DAD contains chlorogenic acid,

p-coumaric acid, rutin, and caffeic acid [26]. Our study revealed that PPE promoted lipolysis in mature adipocytes, as indicated by increased glycerol release, and inhibited lipid accumulation in 3T3-L1 cells, as shown by Oil Red O staining. Gene expression analysis revealed a complex effect: Early adipogenic genes including FAS, ACC1, GLUT4, and C/EBPα were upregulated, while mature adipocyte markers such as adiponectin, FABP4, and CD36 were downregulated. This suggests that PPE allows initiation of the adipogenic program but prevents cells from reaching full maturity, indicative of a metabolic reprogramming effect. Regarding the mechanism of action, the observed anti-adipogenic and pro-lipolytic effects might be linked to the actions of chlorogenic acid (CGA) and p-coumaric acid (PCA) present in PPE. CGA inhibits adipocyte differentiation by activating the AMP-activated protein kinase (AMPK) pathway, which suppresses key transcription factors C/EBPα and PPARγ, while simultaneously activating the Nrf2 pathway to enhance antioxidant enzyme expression (SOD, CAT, GSH-Px), reducing ROS and promoting lipolysis [27]. PCA from *Sasa quelpaertensis Nakai* extract similarly downregulates C/EBPα, PPARγ, and SREBP-1c, activates AMPK to enhance ACC phosphorylation and fatty acid oxidation, and promotes mitochondrial biogenesis and browning of white adipocytes, increasing energy expenditure [28]. These pathways collectively explain PPE's dual mechanism of reducing lipid storage and enhancing lipid breakdown in adipocytes. In addition, PPE decreased intracellular ROS levels in differentiated cells, mitigating oxidative stress, which is known to impair insulin signaling, GLUT4 translocation, and key lipogenic enzymes such as FAS and ACC1 [29,30]. Downregulation of CD36 further reduces fatty acid uptake, limiting lipid accumulation despite upregulation of lipogenic enzymes. Together, these effects indicate that PPE exerts anti-obesity effects by simultaneously modulating oxidative stress, adipogenic differentiation, and lipolytic pathways. Although PPE showed potent *in vitro* activity, future studies should explore the physiological relevance of these concentrations, bioavailability, and *in vivo* efficacy. Additionally, direct assessment of AMPK, PPARγ, and Nrf2 activation, as well as mitochondrial activity, would further clarify the molecular mechanisms of PPE.

Conclusions

PPE's anti-adipogenic effect is not due to a simple downregulation of genes. Instead, it operates through a unique, multifaceted mechanism that suppresses key mature adipocyte markers and uncouples metabolic processes, all while providing antioxidant protection likely mediated by its phenolic constituents (CGA and PCA). These findings highlight PPE as a promising natural candidate for dietary supplementation or therapeutic development against obesity. However, future research should elucidate how PPE modulates key adipogenic and lipolytic genes while simultaneously regulating oxidative stress.

Acknowledgements

This work was supported by (i) Faculty of Sciences, Prince of Songkla University (Grant No: SCI6504007S), Thailand and (ii) Prince of Songkhla University (Grant No: SCI6502074S), Songkhla 90110, Thailand.

Declaration of Generative AI in Scientific Writing

The authors acknowledge the use of generative AI tools (e.g., ChatGPT by OpenAI) in the preparation of this manuscript, specifically for language editing and grammar correction. No content generation or data interpretation was performed by AI. The authors take full responsibility for the content and conclusions of this work.

CRediT Author Statement

Aekkaraj Nuallaong: Methodology; Software; Investigation; Resources; Writing - Original draft preparation. **Benjawan Dunkhunthod:** Methodology; Resources; Writing - Original draft preparation. **Gordon Lowe:** Supervision; Conceptualization; Writing - Review & Editing. **Kornsuda Thipart:** Methodology; Software; Resources; Writing - Original draft preparation; Visualization. **Tanaporn Hengpratom:** Investigation; Conceptualization; Methodology; Data curation; Validation; Writing - Reviewing and Editing; Project administration; Funding acquisition.

References

[1] Y Zhang, J Liu, J Yao, G Ji, L Qian, J Wang, G Zhang, J Tian, Y Nie, YE Zhang, MS Gold and Y Liu. Obesity: Pathophysiology and intervention. *Nutrients* 2014; **6(11)**, 5153-5183.

[2] X Jin, T Qiu, L Li, R Yu, X Chen, C Li, CG Proud and T Jiang. Pathophysiology of obesity and its associated diseases. *Acta Pharmaceutica Sinica B* 2023; **13(6)**, 2403-2424.

[3] K Lee, L Kruper, CM Dieli-Conwright and JE Mortimer. The impact of obesity on breast cancer diagnosis and treatment. *Current Oncology Reports* 2019; **21**, 41.

[4] KA Orringer, RV Harrison, SS Nichani, MA Riley, AE Rothberg, LE Trudeau and Y White. *Obesity prevention and management*. Michigan Medicine University of Michigan, Michigan, 2020.

[5] ED Rosen and BM Spiegelman. What we talk about when we talk about fat. *Cell* 2014; **165(1-2)**, 20-44.

[6] J Jakab, B Miskic, S Miksic, B Juranic, V Cosic, D Schwarz and A Vcev. Adipogenesis as a potential anti-obesity target: A review of pharmacological treatment and natural products. *Diabetes, Metabolic Syndrome and Obesity: Targets and Therapy* 2021; **14**, 67-83.

[7] XD Yang, XC Ge, SY Jiang and YY Yang. Potential lipolytic regulators derived from natural products as effective approaches to treat obesity. *Frontiers in Endocrinology* 2022; **13**, 1000739.

[8] A Yang and EP Mottillo. Adipocyte lipolysis: From molecular mechanisms of regulation to disease and therapeutics. *Biochemical Journal* 2020; **477(5)**, 985-1008.

[9] M Rajendran, S Palani, TG Singh, B Oliver, K Dua, V Subramaniyan and K Narayanan. The dual role of conjugated linoleic acid in obesity and metabolic disorders. *Food Science & Nutrition* 2025; **13(7)**, 70582.

[10] K Chayarop, R Temsiririrkkul, P Peungvicha, Y Wongkrajang, W Chuakul, S Amnuoypol and N Ruangwises. Antidiabetic effects and in vitro antioxidant activity of *Pseuderanthemum palatiferum* (Nees) Radlk. ex Lindau leaf aqueous extract. *Mahidol University Journal of Pharmaceutical Science* 2011; **38(3-4)**, 13-22.

[11] P Komonrit and R Banjerdpongchai. Effect of *Pseuderanthemum palatiferum* (Nees) Radlk fresh leaf ethanolic extract on human breast cancer MDA-MB-231 regulated cell death. *Tumor Biology* 2018; **40(9)**, 1010428318800182.

[12] P Padee, S Nualkaew, C Talubmook and S Sakuljaitrong. Hypoglycemic effect of a leaf extract of *Pseuderanthemum palatiferum* (Nees) Radlk. in normal and streptozotocin-induced diabetic rats. *Journal of Ethnopharmacology* 2010; **132(2)**, 491-496.

[13] T Khumpook, S Chomdej, S Saenphet, D Amornlerdpison and K Saenphet. Anti-inflammatory activity of ethanol extract from the leaves of *Pseuderanthemum palatiferum* (Nees) radlk. *Chiang Mai Journal of Science* 2013; **40(3)**, 321-331.

[14] K Chayarop, P Peungvicha, Y Wongkrajang, W Chuakul, S Amnuoypol and R Temsiririrkkul. Pharmacognostic and phytochemical investigations of *Pseuderanthemum palatiferum* (Nees) radlk. ex Lindau Leaves. *Pharmacognosy Journal* 2011; **3(23)**, 18-23.

[15] P Sittisart, B Chitsomboon and NE Kaminski. *Pseuderanthemum palatiferum* leaf extract inhibits the proinflammatory cytokines, TNF-α and IL-6 expression in LPS-activated macrophages. *Food and Chemical Toxicology* 2016; **97**, 11-22.

[16] P Sittisart and B Chitsomboon. Intracellular ROS scavenging activity and downregulation of inflammatory mediators in RAW264.7 macrophage by fresh leaf extracts of *Pseuderanthemum palatiferum*. *Evidence-Based Complementary and Alternative Medicine* 2014; **2014**, 309095.

[17] KJ Livak and TD Schmittgen. Analysis of relative gene expression data using real-time quantitative PCR and the 2(-Delta Delta C(T)) Method. *Methods* 2001; **25(4)**, 402-408.

[18] B Dunkhunthod, C Talabnin, M Murphy, K Thumanu, P Sittisart and G Eumkeb. *Gymnema inodorum* (Lour.) Decne. extract alleviates oxidative stress and inflammatory mediators produced by RAW264.7 macrophages. *Oxidative Medicine and Cellular Longevity* 2021; **2021**, 8658314.

[19] JJ Fuster, N Ouchi, N Gokce and K Walsh. Obesity-Induced changes in adipose tissue microenvironment and their impact on cardiovascular disease. *Circulation Research* 2016; **118(11)**, 1786-1807.

[20] UFSM Sayed, S Moshawih, HP Goh, N Kifli, G Gupta, SK Singh, DK Chellappan, K Dua, A Hermansyah, HL Ser, LC Ming and BH Goh. Natural products as novel anti-obesity agents: Insights into mechanisms of action and potential for therapeutic management. *Frontiers in Pharmacology* 2023; **14**, 1182937.

[21] P Padee, S Nualkaew, C Talubmook and S Sakuljaitrong. Hypoglycemic effect of a leaf extract of *Pseuderanthemum palatiferum* (Nees) radlk. in normal and streptozotocin-induced diabetic rats. *Journal of Ethnopharmacology* 2010; **132(2)**, 491-496.

[22] P Padee, S Nualkaew, C Talubmook and S Sakuljaitrong. Acute toxicity and sub-acute toxicity of *Pseuderanthemun palatiferum* (Nees) radlk. Leaf Extract. *Isan Journal of Pharmaceutical Sciences* 2009; **5(1)**, 74-81.

[23] YH Kim, DH Kim, H Lim, DY Baek, HK Shin and JK Kim. The anti-inflammatory effects of methylsulfonylmethane on lipopolysaccharide-induced inflammatory responses in murine macrophages. *Biological and Pharmaceutical Bulletin* 2009; **32(4)**, 651-656.

[24] I Sousa-Lima, SY Park, M Chung, HJ Jung, MC Kang, JM Gaspar, JA Seo, MP Macedo, KS Park, C Mantzoros, SH Lee and YB Kim. Methylsulfonylmethane (MSM), an organosulfur compound, is effective against obesity-induced metabolic disorders in mice. *Metabolism* 2016; **65(10)**, 1508-1521.

[25] JB Jeong, SC Hong, HJ Jeong and JS Koo. Anti-inflammatory effect of 2-methoxy-4-vinylphenol via the suppression of NF-κB and MAPK activation, and acetylation of histone H3. *Archives of Pharmacal Research* 2011; **34(12)**, 2109-2106.

[26] V Danh, N Trang and XT Vo. Influence of green solvent extraction on phytochemicals, potential antidiabetic and *in vitro* anti-inflammatory activities of *Pseuderanthemum palatiferum* (Nees.) Radlk. Leaves. *The Tropical Journal of Natural Product Research* 2023; **7(1)**, 2215-2219.

[27] LV Vasileva, MS Savova, KM Amirova, Z Balcheva-Sivenova, C Ferrante, G Orlando, M Wabitsch and MI Georgiev. Caffeic and chlorogenic acids synergistically activate browning program in human adipocytes: Implications of AMPK- and PPAR-Mediated pathways. *International Journal of Molecular Sciences* 2020; **21(24)**, 9740.

[28] SW Kang, SI Kang, HS Shin, SA Yoon, JH Kim, HC Ko and SJ Kim. *Sasa quelpaertensis* Nakai extract and its constituent p-coumaric acid inhibit adipogenesis in 3T3-L1 cells through activation of the AMPK pathway. *Food and Chemical Toxicology* 2013; **59**, 380-385.

[29] B Ahmad, CJ Serpell, IL Fong and EH Wong. Molecular mechanisms of adipogenesis: The anti-adipogenic role of AMP-Activated protein kinase. *Frontiers in Molecular Biosciences* 2020; **7**, 76.

[30] P Jimenez-Quevedo, A Serrador, AP de Prado, L Nombela-Franco, C Biagioni and M Pan. Selection of the best of 2016 in interventional cardiology: Expansion of TAVI indications to intermediate-risk patients. *Revista Española de Cardiología* 2017; **70(3)**, 218-219.

Supplementary Material

Potential Effects of *Pseuderanthemum palatiferum* Extract on Inhibiting Adipogenesis and Promoting Lipolysis in 3T3-L1 Cell line

Supplementary data

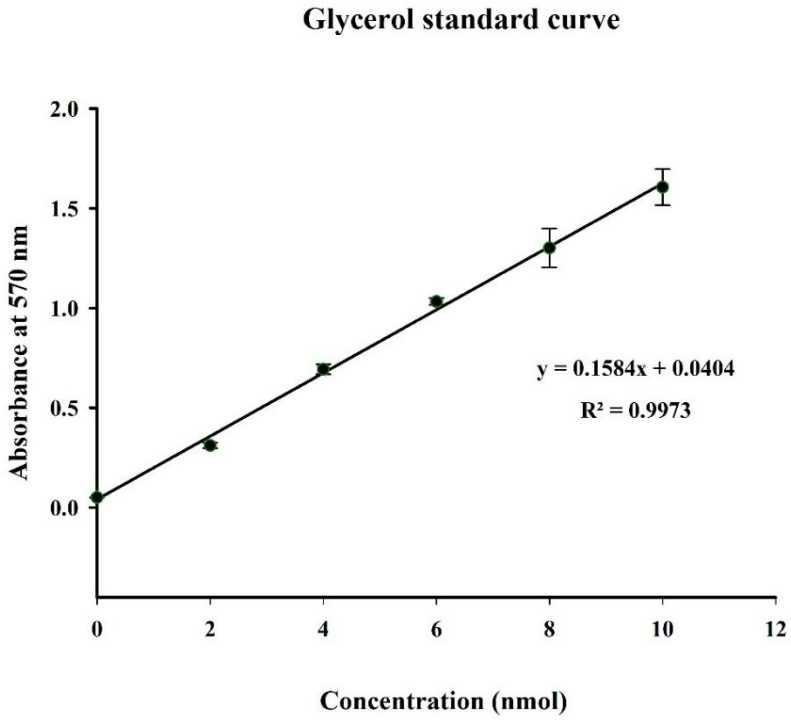

Supplementary data 1 Standard curve for determination of glycerol releasing level of PPE.

Supplementary data 2 Primer sets for RT-qPCR.

Gene name	Forward primer sequence (5'->3')	Reverse primer sequence (5'->3')	Annealing temperature (°C)
β-actin1	CAGCTGAGAGGGAAATCGTG	CGTTGCCAATAGTGATGACC	57.0
GLUT4	GTGACTGGAACACTGGTCCTA	CCAGCCACGTTGCATTGTAG	59.0
fasn	GCCCAAGGGAAGCACATT	CGAAGCCATTTAGACCAC	55.0
acc1	AAAACAGGGAGGAACGAA	TCACCCCGAATAGACAGC	55.0
c/ebp α	CTGGAAAGAAGGCCACCTC	AAGAGAAGGAAGCGGTCCA	59.0
srebp1c	GCAACACAGCAACCAGAA	GAAAGGTGAGCCAGCAT	59.0
Adiponectin	TGTTCCTCTTAATCCTGCCCA	CCAACCTGCACAAGTTCCCTT	63.3
AP2	AAGGTGAAGAGCATCATAACCCT	TCACGCCTTTCATAACACATTCC	63.3
LPL	GGGAGTTTGGCTCCAGAGTTT	TGTGTCTTCAGGGGTCCTTAG	59.0
CD36	AAGCTATTGCGACATGATT	GATCCGAACACAGCGTAGAT	59.0
SCD1	ATGCCGGCCCACATGCTCCA	CATGAGGATGATGTTCCTCC	59.0

Supplementary data 3 Gas chromatography/mass spectrometry (GC-MS) profile of PPE.

Peak number	Compound	Retention time	Peak area (%)	Quality
1	cis-Aconitic anhydride	31.52	0.94	84.1
2	2(5H)-Furanone	31.76	0.39	81.6
3	2-Hydroxy-2,5-dimethyl-hept-6-en-3-one	32.04	1.47	67.5
4	Methyl salicylate	32.31	1.13	72.3
5	1,2-Cyclopentanedione, 3-methyl-	33.86	0.21	41.8
6	N,N-Dimethyl-2-methoxyethylamine	34.2	3.58	52.8
7	Phenol, 2-methoxy-	34.57	3.25	55.7
8	Benzyl alcohol	35.16	0.55	43
9	Dimethyl sulfone	36.05	21.63	68.2
10	S-Methyl methanethiosulphonate	38.26	0.58	86
11	2H-Pyran-2,6(3H)-dione	38.75	0.36	91.5
12	Phenol	39.09	1.88	52
13	3-Furancarboxylic acid, methyl ester	39.32	0.41	30.2
14	2,5-Dimethyl-4-hydroxy-3(2H)-furanone	40.32	1.24	66.7
15	Piperidine, 1-nitroso-	42.87	0.38	48.6
16	Phenol, 2-ethyl-	44.38	1.23	17.1
17	2-Methoxy-4-vinylphenol	45.02	11.58	49.2
18	Phenol, 2,6-dimethoxy-	47.16	2.33	71.5
19	Pyranone	47.34	2.04	94.2
20	Megastigmatrienone	48.88	0.98	43.8
21	trans-Isoeugenol	49.85	0.69	19.8
22	Benzofuran, 2,3-dihydro-	51.19	29.94	41.9
23	Benzoic acid	52.32	0.77	21.8
24	Indole	52.62	0.78	53.3
25	(S)-(+)-2',3'-Dideoxyribonolactone	54.01	0.73	56.7
26	Phenol, 4-(2-propenyl)-	54.88	1.34	49.2
27	2-(3,4-Dimethoxyphenyl)-6-methyl-3,4-chromanediol	56.26	1.37	29.6
28	Benzenepropanoic acid 1-methylethyl ester	57.35	1.24	13.1
29	5-Oxotetrahydrofuran-2-carboxylic acid	57.79	0.37	23.4
30	Catechol	58.95	2.83	79.1
31	Methoxyeugenol	59.7	0.58	65.9
32	4-Ethylcatechol	62.53	1.19	39.8
33	n-Hexadecanoic acid	63.76	0.35	47.2
34	1,4-Benzenediol, 2-methoxy-	64.8	0.50	36.8
35	Hydroquinone	66.48	1.17	47.6